

On the properties of superconducting planar resonators at mK temperatures

T. Lindström,* J.E. Healey, M.S. Colclough, and C.M. Muirhead
University of Birmingham, Edgbaston, Birmingham B15 2TT, UK[†]

A.Ya.Tzalenchuk
National Physical Laboratory, Hampton Road, Teddington, TW11 0LW, UK
(Dated: December 4, 2018)

Planar superconducting resonators are now being increasingly used at mK temperatures in a number of novel applications. They are also interesting devices in their own right since they allow us to probe the properties of both the superconductor and its environment. We have experimentally investigated three types of niobium resonators - including a lumped element design - fabricated on sapphire and SiO₂/Si substrates. They all exhibit a non-trivial temperature dependence of their centre frequency and quality factor. Our results shed new light on the interaction between the electromagnetic waves in the resonator and two-level fluctuators in the substrate.

I. INTRODUCTION

The superconducting microwave resonator is an ubiquitous device with uses ranging from the very practical - such as filters for telecommunications - to rather exotic such as tests of cavity quantum electrodynamics. Over recent years there has been a resurgence in the interest in on-chip resonators; the primary reason being their use as very sensitive photon and much of the work to date has been motivated by the need to understand noise properties of kinetic inductance detectors (KID)^{1,2,3}. Resonators are also being used as elements in circuitry for quantum information processing⁴. The latter has triggered a wave of investigations into the properties of resonators when operated at mK temperatures and very low (ideally single photon) microwave powers. Of particular interest has been the effects of two-level fluctuators (see e.g.^{5,6} and references therein). Superconducting resonators at microwave frequencies differ from their normal metal counterparts primarily because of their high quality factor (Q) and a relatively large kinetic inductance. For example, for an ideal high-Q LC resonator we can write the centre frequency as $f_0 = (2\pi\sqrt{(L + L_K)C})^{-1}$ where L_K is the contribution from the kinetic inductance. L_K depends on the order parameter and therefore varies with temperature, but can also be altered e.g. by a weak magnetic field⁷. As the temperature goes down the centre frequency increases monotonically while the conductor losses decrease (leading to a higher quality factor), as described by the Mattis-Bardeen theory⁸. However, at temperatures $\sim T_c/10$, these mechanisms saturate (in Nb and its compounds around 1 K) and other effects become prominent^{1,3,7}, most notably a *decrease* in the centre frequency as the temperature is reduced. This 'back-bending' is now widely believed to be due to the presence of two-level fluctuators (TLF) in the substrate.

Here we will discuss measurements of the centre frequency and losses in three types of Nb resonators: conventional $\lambda/2$ and $\lambda/4$ geometric resonators and a recently developed type of lumped element resonator⁹.

II. THEORY

A generic expression for the transmittance, S_{21} , of a transmission line shunted by a resonator (e.g. the lumped element and $\lambda/4$ resonators considered here) can be written $S_{21} = 2 \left[2 + \frac{g}{1+2jQ_u\delta f} \right]^{-1}$ where Q_u is the unloaded quality factor (Q in the absence of coupling to the feed-line), g is a coupling parameter $\propto Q_u$ - the exact expression for which will depend on the type of resonator used- and $\delta f = (f - f_0)/f_0$ is the fractional shift from resonance. The value of Q_u is in general given by summing over all loss mechanisms $\sum_k Q_k^{-1}$ but losses in the dielectric and the superconducting film itself¹⁰ usually dominate in planar resonators and radiation losses etc. can be neglected. Microwave losses are usually quantified by the loss tangent $\tan \delta = 1/Q_u$, which in a dielectric is proportional to the sum of the various absorption mechanisms $\sum_k \alpha_k$.

At sub-Kelvin temperatures one would expect the properties of a dielectric to stay essentially constant. However, experimentally one finds a variation in both the effective dielectric constant and losses. Much of this can be explained if one assumes the presence of a bath of TLF that couple to the resonator via their electric dipole moment. Many of the details of the corresponding theory were worked out over 30 years ago when the effects of TLF in glasses at low temperatures were being investigated¹¹. The theory is based on the application of the Bloch equations to an ensemble of spin systems and while it is simple it nevertheless captures most of the essential physics. For resonant absorption due to an ensemble of TLF α_r has the form^{12,13}

$$\alpha_r = \frac{\pi\omega nd^2}{3c_0\epsilon_0\epsilon_r} \left(1 + \frac{P}{P_c} \right)^{-1/2} \tanh \left(\frac{\hbar\omega}{2k_B T} \right) \quad (1)$$

where ω is the measurement frequency, d is the dipole moment, c_0 is the speed of light in vacuum and n is the density of states of the TLF that couple to the stray field of the resonator. Note that this density should in principle depend on frequency, but is experimentally of-

ten found to be constant. The temperature dependence of the absorption reflects the population difference of the two states of the fluctuators, as the temperature increases the TLF will therefore absorb *less* power. Note that Eq. 1 only accounts for *resonant* absorption, non-resonant relaxation processes due the TLF bath are not taken into account.

The relation above predicts a power dependence of the absorption $\propto P^{-1/2}$ above some critical power P_c , although in practice one may expect another high-power roll-off once all the TLF are saturated and other loss mechanisms start to dominate. The critical intensity is given by $P_c = 3\hbar^2 c_0 \epsilon_0 \epsilon_r / 2d^2 T_1 T_2$ where T_1 and T_2 are the relaxation and the dephasing times of the TLF, respectively.

The variation in permittivity is dominated by resonant processes and can therefore be found by applying the Kramers-Kronig relations to Eq.1

$$\frac{\epsilon(T) - \epsilon(T_0)}{\epsilon(T_0)} = -\frac{2nd^2}{3\epsilon} \left[\ln\left(\frac{T}{T_0}\right) - (g(T, \omega) - g(T_0, \omega)) \right] \quad (2)$$

where $g(T, \omega) = \text{Re}\Psi(\frac{1}{2} + \hbar\omega/2\pi i k_B T)$, T_0 is a reference temperature and Ψ the complex digamma function significant only for $kT \lesssim \hbar\omega/2$. From cavity perturbation theory we then have that $\Delta f_0/f_0 = -F/2\Delta\epsilon/\epsilon$, F being a filling factor which depends on the geometry and the electric field distribution. The substrate filling factor varies slightly between the three types of resonator discussed here; but is over 0.9 in all cases. For samples on SiO_2/Si substrates the contribution of the SiO_2 layer to F is about 0.2. Eq. 1 predicts an upward turn in the temperature dependence of the centre frequency at mK temperatures, where the $g(T, \omega)$ term is important. In the experiments by Gao *et al*¹⁴ Eq. 2 was used to fit the temperature dependence of the resonance frequency, but the low-temperature upturn was not clearly observed.

The aim of this experimental study is to verify whether the theory developed for a spin solution in glass can accurately describe the temperature and power dependence of the resonance frequency and losses in superconducting resonators at mK temperatures.

III. EXPERIMENTAL

We have fabricated a wide variety of $\lambda/2$, $\lambda/4$ and lumped element (LE) niobium resonators (see fig. 1) on R-cut sapphire and thermally oxidized high-resistivity ($> 1 \text{ k}\Omega/\text{cm}^2$) silicon substrates with 400 nm of SiO_2 . The simplest design is the in-line $\lambda/2$ resonator. Its advantages is that it can be made with loaded quality factors of $> 10^6$ and is easy to measure (due to the high S/N ratio on resonance), there is however only one resonator per chip and a calibrated measurement is needed in order to quantify its unloaded quality factor (which is difficult at mK temperatures). $\lambda/4$ resonators have the advantage that their parameters can be extracted rela-

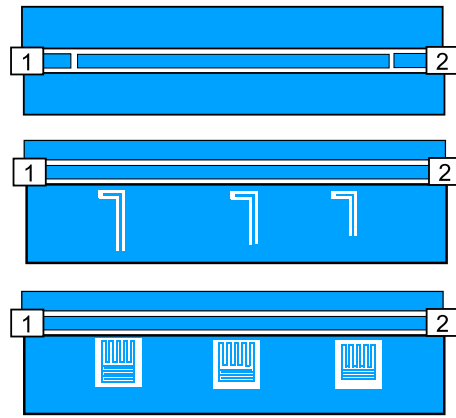


FIG. 1: Illustration (*not to scale*) showing the geometry and measurement configuration (ports $2 \rightarrow 1$) for the three types of resonators used in this work. From top to bottom: $\lambda/2$, $\lambda/4$ and Lumped element (LE) resonator.

tively easily (using numerical fitting) from uncalibrated measurements since the transmittance far from resonance can be used as a reference level. Several $\lambda/4$ resonators can be coupled to a common feedline, making it possible to measure in a frequency-multiplexed configuration. The lumped element resonator shares these advantages and is much more compact (typical size is about $200 \times 200 \mu\text{m}^2$) than geometric resonators. Our LE resonators fabricated in Nb on sapphire exhibit loaded Q close to 10^5 with an unloaded Q that is about 3 times higher; i.e the resonators are by design overcoupled.

The structures were patterned in 200 nm thick sputtered Nb films using ion-beam etching and were designed to have their centre frequencies in the c-band(4-8 GHz). Table I shows a summary of the samples discussed in this paper. Other resonators measured to-date showed similar behaviour. Each chip is $5 \times 10 \text{ mm}^2$ in size and incorporates a central 50Ω coplanar feed-line and one or more resonators. For the measurement the chip is glued to a gold-plated alumina carrier inside a superconducting box. All measurements (with the exception for the data above

TABLE I: Summary of the resonators used in these experiments presented in this paper

	Type	Chip	Substrate	f_0 at 50 mK (MHz)
R1	$\lambda/2^a$	A	SiO_2/Si	6037
R2	$\lambda/4$	B	SiO_2/Si	5040
R3	$\lambda/4$	B	SiO_2/Si	5795
R4	$\lambda/4$	B	SiO_2/Si	8100
R5	LE	C	SiO_2/Si	6805
R6	LE	C	SiO_2/Si	7250
R7	LE	C	SiO_2/Si	7813
R8	LE	D	Sapphire	6046
R9	LE	D	Sapphire	6458
R10	LE	D	Sapphire	6959

^aSingle resonator on the chip, measured in-line

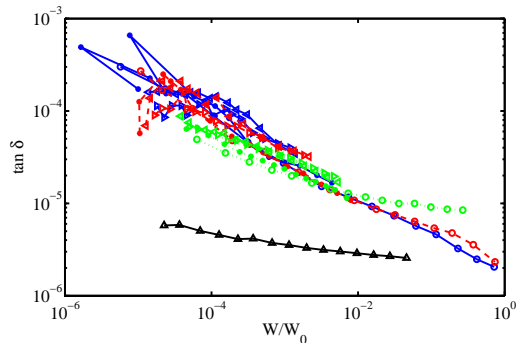


FIG. 2: Loss tangent for 3 lumped element resonators (R5-R7: green dotted, red dashed and solid blue line, respectively) on SiO₂/Si at 4 different temperatures: 50mK(○), 100mK (*), 250mK(◀) and 340mK(▶). The lowest curve (▲) shows a similar measurement at 30mK for R8, a resonator on sapphire. All curves were measured using the same *applied* power.

1 K in fig. 4) were carried out in a dilution refrigerator with heavily filtered microwave lines. The transmitted signal was amplified using an InP HEMT amplifier held at 1 K with a noise temperature of about 4 K, before further amplification stages at room temperature.

IV. RESULTS AND DISCUSSION

Figure 2 shows how the loss tangent depends on the energy in the resonator on resonance $W = 2Q_u(1 - S_{21})S_{21}P_{in}/\omega_0$ for three different lumped element resonators on SiO₂/Si coupled to the same on-chip transmission line and measured simultaneously. Absolute power metrology at mK temperatures is very problematic so only relative measurements were possible; we estimate that the maximum power reaching the chip during the measurements is about -70 dBm, meaning W_0 is of the order of 10^{-16} Ws. Shown is also R8, a sapphire resonator of the same design. For the resonators fabricated on SiO₂/Si the curves have a slope of approximately -0.4 in this range of applied powers. Eq. 1 predicts dielectric losses changing with a slope of -0.5 for powers above P_c and power-independent behavior below P_c , it is therefore possible that we are in the intermediate regime. However, it is also possible that losses in the superconductor not captured by Eq. 1 play a role. Indeed, the current distribution in superconducting resonators is such that its *local* value can be significant even at our lowest powers leading to higher conductor losses as the power is increased. It is also interesting to note that the power entering the resonator depends on Q and Q -due to the TLF- in turn depends on the power, $Q \propto P(Q)$. Hence, the system is non-linear and in principle weakly hysteretic.

The main conclusion from fig. 2 is that the loss tangent is strongly power dependent for SiO₂/Si whereas a weak dependence is observed for identical structures on sapphire; in the latter case Q only changes by about a

factor of two even when the power is changed by over 40 dB.

Experimentally, the temperature dependence of the resonance frequency of superconducting resonators is quite complicated since it is affected both by the properties of the superconducting film (e.g. the kinetic inductance) and changes in the dielectric and it is in general difficult to separate these two effects. However, at temperatures $\ll T_c$, which is the case here, we can assume that the thermal effects on the kinetic inductance are small. Figure 3 shows the relative shift of the resonance frequency as a function of $\hbar\omega/k_B T$ together with a fit to Eq. 2. All data from the resonators on a particular substrate can be fitted using a single parameter; we find $Fd^2n/3\epsilon = 6 \cdot 10^{-5}$ and $2.8 \cdot 10^{-6}$ for the SiO₂/Si and sapphire respectively; a difference of about a factor of twenty; consistent with the loss tangent measurements. Note that the curves shown come from several resonators of two different designs (on separate chips), with each resonator measured at several different power levels, but they can all be fitted using a single parameter. We note that the values for $Fd^2n/3\epsilon$ we obtain from samples fabricated on sapphire are consistently lower than those reported by Gao *et al.*

In order to verify that the temperature dependence does not depend on the geometry or our data analysis, we have in addition to lumped-element and $\lambda/4$ (in shunt configuration) resonators also measured undercoupled in-line $\lambda/2$ coplanar resonators. Fig. 4 shows the measured temperature dependence of $1/Q_l - Q_l$ being the loaded quality factor- and f_0 . Again we can fit all the f_0 curves

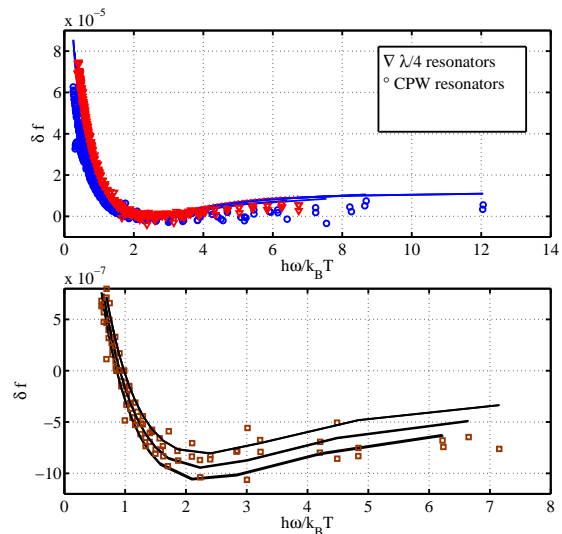


FIG. 3: Frequency shift as a function of the normalized frequency at several different powers for LE resonators R2 to R7 on SiO₂/Si (*top*); and R8 to R10 sapphire(*bottom*). The solid lines show fits to theory. The log term dominates at small $\hbar\omega/k_B T$ whereas $g(t)$ becomes important in the opposite regime. Successive curves differ in power by 10 dB.

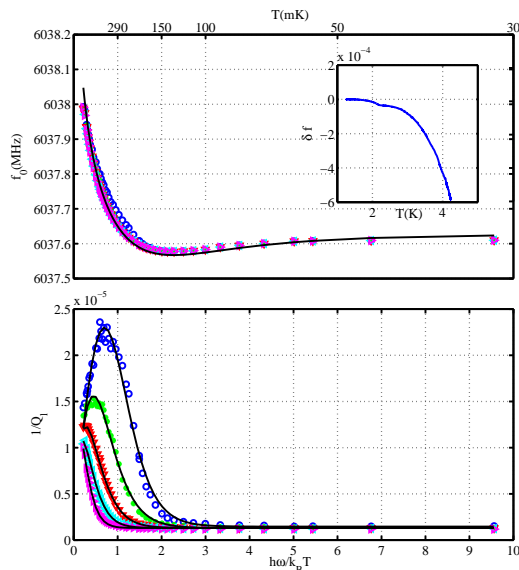


FIG. 4: Centre frequency (*Top*) and $1/Q_l$ (*Bottom*) at five different powers and as a function of temperature for sample R1, a $\lambda/2$ resonator fabricated on SiO_2/Si . Each successive curve (top to bottom) corresponds to an increase in power by 2 dB. Solid curves show fit to theory. *Inset*: $\lambda/2$ resonator measured above 1K.

using a single parameter, although in this case the fitting parameter $Fd^2n/3\epsilon$ is $4.95 \cdot 10^{-5}$, slightly lower than for the other samples. Some of this difference is likely to be due to somewhat different filling factors.

At temperatures above 1K the losses are dominated by the conductor losses described by the Mattis-Bardeen theory but at low temperatures and low microwave power conductor losses are no longer important; resonant absorption dominates and the losses increase as the temperature is reduced as captured by Eq.1. High power on the other hand saturates the TLS thus suppressing the resonant absorption. Fig. 4 (*bottom*) illustrates the regime of decreasing losses at temperatures below about 300 mK, which can only be observed in a very narrow range of microwave power. This regime is obviously not described by resonant absorption Eq. 1. The likely ex-

planation is that the relative significance of *relaxation* absorption¹⁵ processes increases for temperatures below $\approx \hbar\omega/k_B$ and intermediate power levels, just enough to suppress the resonant absorption. As the power is increased, the crossover to the relaxation losses is pushed to higher temperatures.

Whilst the presence of TLF is known to affect resonators it is nevertheless surprising how well our data can be fitted using a single parameter independent of both the frequency (over a range of several GHz) and the location on the chip. While our data do not give us a reliable way to identify the nature of these TLF, one can with some certainty conclude that their origin must somehow be intrinsic to the materials used. The bath of TLF appears to have a very wide distribution of both the tunnel splittings and the symmetry parameter of the (effective) double-well. The large nd^2 factor in SiO_2/Si -consistent with previous measurements¹⁶- comes as no surprise given the large density of TLF one would expect in an amorphous oxide material. The nd^2 factor in sapphire is significantly smaller, but still measurable. This is in itself quite interesting as it is well known that the only two-levels systems seen in very high-quality dielectric sapphire resonators are known to be due to -relatively narrow- electron spin resonances on incidental paramagnetic ions, such as Fe or Cr; if these were the origin of the TLF in our samples one would not expect the data to agree with the theory used here. This suggests that the TLF seen here are located in the interface between the film and the substrate, as opposed to the bulk material.

Acknowledgments

We wish to acknowledge John Gallop, Yuri Galperin, Gregoire Ithier, Olga Kazakova, Phil Mauskopf, Phil Meeson, Mark Oxborrow, Giovanna Tancredi and members of NTT Basic Research Laboratories for helpful discussions and comments. This work was supported by EPSRC and the the National Measurement Programme of the Department for Industries, Universities and Skills (DIUS).

* Electronic address: tobias.lindstrom@npl.co.uk

† Also at National Physical Laboratory, Hampton Road, Teddington, TW11 0LW, UK

¹ J. Gao, J. Zmuidzinas, B. Mazin, H. LeDuc, and P. Day, Applied Physics Letters **90**, 102507 (2007).

² S. Kumar, J. Gao, J. Zmuidzinas, B. Mazin, H. LeDuc, and P. Day, Applied Physics Letters **92**, 123503 (2008).

³ R. Barends, H. L. Hortensius, T. Zijlstra, J. J. A. Baselmans, S. J. C. Yates, J. R. Gao, and T. M. Klapwijk, Applied Physics Letters **92**, 223502 (2008).

⁴ A. Wallraff, D. Schuster, A. Blais, L. Frunzio, R. Huang, J. Majer, S. Kumar, S. Girvin, and R. Schoelkopf, Nature

431, 162 (2004).

⁵ J. Clarke and F. K. Wilhelm, Nature **453**, 1031 (2008).

⁶ L. Faoro, A. Kitaev, and L. B. Ioffe, Physical Review Letters **101**, 247002 (2008).

⁷ J. E. Healey, T. Lindstrom, M. S. Colclough, C. M. Muirhead, and A. Y. Tzalenchuk, Applied Physics Letters **93**, 3 (2008).

⁸ D. Mattis and J. Bardeen, Physical Review **111**, 412 (1958).

⁹ S. Doyle, P. Mauskopf, J. Naylon, A. Porch, and C. Duncombe, J. Low Temperature Physics. pp. 530–536 (2008).

¹⁰ C. Song, T. W. Heitmann, M. P. DeFeo, K. Yu, R. Mc-

- Dermott, M. Neeley, J. M. Martinis, and B. L. T. Plourde, arXiv.org:0812.3645 (2008).
- ¹¹ W. A. Phillips, Rep. Prog. Phys **50**, 1657 (1987).
- ¹² U. Strom, M. von Schickfus, and S. Hunklinger, Physical Review Letters **41**, 910 (1978).
- ¹³ M. von Schickfus and S. Hunklinger, Physics Letters **64A**, 144 (1977).
- ¹⁴ J. Gao, M. Daal, A. Vayonakis, S. Kumar, J. Zmuidzinas, B. Sadoulet, B. A. Mazin, P. K. Day, and H. G. Leduc, Applied Physics Letters **92**, 152505 (pages 3) (2008).
- ¹⁵ Y. Galperin, V. Gurevich, and D. Parshin, in *Hopping Transport in Solids*, edited by B. Shklovskii and M. Polak (Elsevier, 1991), chap. Non-Ohmic microwave hopping conductivity.
- ¹⁶ A. O'Connell, M. Ansmann, R. Bialczak, M. Hofheinz, N. Katz, E. Lucero, C. McKenney, M. Neeley, H. Wang, and E. Weig, Applied Physics Letters **92**, 112903 (2008).